ward shift of the postbuckling curves. This is illustrated in Fig. 3. Such a downward shift would explain why σ/σ_{cl} decreases as R/t increases.

Conclusion

The number of circumferential buckling lobes n is a function of L/R and R/t. The nature of this dependency poses a new problem in the understanding of the mechanism of buckling of circular cylinders under axial load. The author is now conducting an extensive series of tests on Mylar cylinders to investigate this mechanism.

References

[1] Wilson, W. N. and Newmark, N. M., "The strength of thin cylindrical shells," Univ. of Illinois Bull. **255** (1933).

[2] Donnell, L. H., "A new theory for the buckling of thin cylinders under axial compression and bending," Trans. Am. Soc. Mech. Engrs. **56**, 795–806 (1934).

[3] Von Karman, T. and Tsien, H.-S., "The buckling of thin cylindrical shells under axial compression," J. Aeronaut. Sci. **8**, 303–312 (1941).

[4] Thielemann, W. F., "On the postbuckling behavior of thin cylindrical shells," NASA TN D-1510, pp. 203–216 (1962).

[5] Ballerstedt, W. and Wagner, H., "Versuche ueber die Festigkeit duenner unversteifter Zylinder unter Schub- und Laengkraeften," Luftfahrtforschung **13**, 309–312 (1936).

Drag on Blunt Bodies with and without Spikes in Low-Density Hypersonic Flow

William H. Sims,* David E. Boylan,† and Jerry S. Hahn‡
ARO Inc., Arnold Air Force Station, Tenn.

Nomenclature

C_∞	=	Chapman-Rubesin constant $(\mu_W T_\infty)/(\mu_\infty T_W)$
$C_D{}^*$	=	normalized drag coefficient $(C_D - C_{D_i})/(C_{D_{FM}} - C_{D_i})$
L	=	see Fig. 1
L_{spike}	=	see Fig. 1
M_∞	=	freestream Mach number
$Re_{\infty,D}$	=	Reynolds number based on body diameter and freestream conditions
$Re_{\infty,L}$	=	Reynolds number based on length L and freestream conditions
T_0	=	reservoir temperature of gas
T_W	=	body wall temperature
$\bar{V}_\infty$	=	viscous interaction drag parameter, $M_\infty(C_\infty/Re_{\infty,L})^{1/2}$

The subject of reducing the drag forces and heating rates by the use of spikes has received much attention in the past.[1–3] Although these studies have encompassed a wide range of Mach number, they have been restricted to conditions of relatively high Reynolds number and do not indicate the viscous interaction effects that planetary entry vehicles encounter at very high altitudes.

For the speed regime of satellite vehicles entering the earth's atmosphere, the necessity of minimizing convective heating led to blunt nose shapes. However, as velocities increase to interplanetary speeds, radiation heating assumes a more important role than does convective heating, reviving interest in the more slender configurations. When the roles of drag coefficient and heat-transfer coefficient are considered in minimizing the ratio of heat transfer to drag coefficients,[4] the desired nose shape then is much more sharp. Because earlier experiments have revealed the effect of low Reynolds number on the drag of a type of blunt body of interest for planetary probes and earth satellites,[5] a program was undertaken to investigate the drag of the same shape after modification to what might be considered a low-drag, low-radiation-heating configuration by addition of a nose spike.[6]

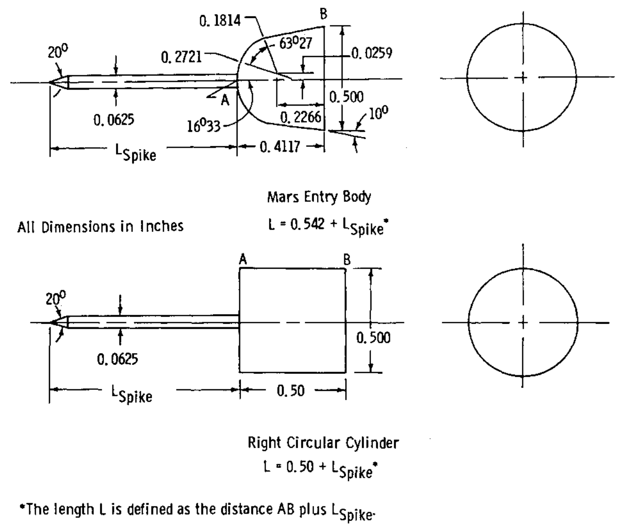

Fig. 1 Model dimensions.

The gas dynamic wind tunnel, Hypersonic (L)[7] of the von Kármán Gas Dynamics Facility, at the Arnold Engineering Development Center, was used. This investigation concerned the aerodynamic drag at various angles of attack for a Mach number of 10.1 and a Reynolds number, based on wetted length, of 200 to 1200. The spike lengths tested varied from 0 to 5.0 body diameters.

The configurations of the models may be seen in Fig. 1. The right circular cylinder was only tested at 0° angle of attack. The data have been reduced to coefficient form and are presented as functions of both L_{spike}/D_{base}, and the viscous interaction parameter

$$\bar{V}_\infty = M_\infty(C_\infty/Re_{\infty,L})^{1/2}$$

where

$$C_\infty = (\mu_W T_\infty)/(\mu_\infty T_W)$$

$$Re_{\infty,L} = U_\infty \rho_\infty L/\mu_\infty$$

and L is the characteristic length as described in Fig. 1. The coefficient $(C_\infty)^{1/2}$ was essentially constant ($\approx$0.83) for this investigation.

Figure 2 indicates the influence of the viscous effects as $\bar{V}_\infty$, α, and L_{spike}/D_{base} vary. Here it may be noted that the reduction in $\bar{V}_\infty$ was a result of the model characteristic length L increasing as spike length increased. Thus, one cannot separate the effects of varying $\bar{V}_\infty$ and L_{spike}/D_{base} in Fig. 2. This is done in a later figure.

The variation of C_D with $\bar{V}_\infty$ for various angles of attack also is shown in Fig. 2. Here a very revealing effect occurs which is undoubtedly due to the predominant viscous effects on the spikes. Whereas in earlier studies reductions in C_D were realized for larger Reynolds numbers even at larger angles of attack when spikes were incorporated in the body, this is no longer true for the present tests. For increasing spike length and angle of attack, above approximately 25° in this particular case, the spike causes drag to increase.

Received August 13, 1964. This work was sponsored by Arnold Engineering Development Center, Air Force Systems Command, U. S. Air Force, under Contract No. AF40(600)-1000.

* Engineer, Research Branch, von Kármán Gas Dynamics Facility. Associate Member AIAA.

† Engineer, Research Branch, von Kármán Gas Dynamics Facility.

‡ Co-op Student, University of Cincinnati and von Kármán Gas Dynamics Facility.

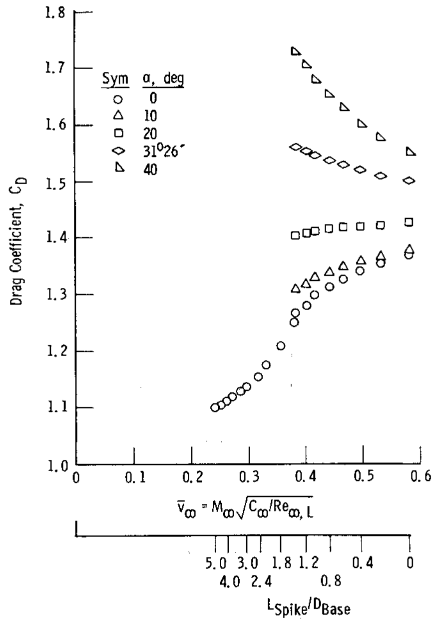

Fig. 2 Drag coefficient as a function of $\bar{V}_\infty$ for varying angle of attack.

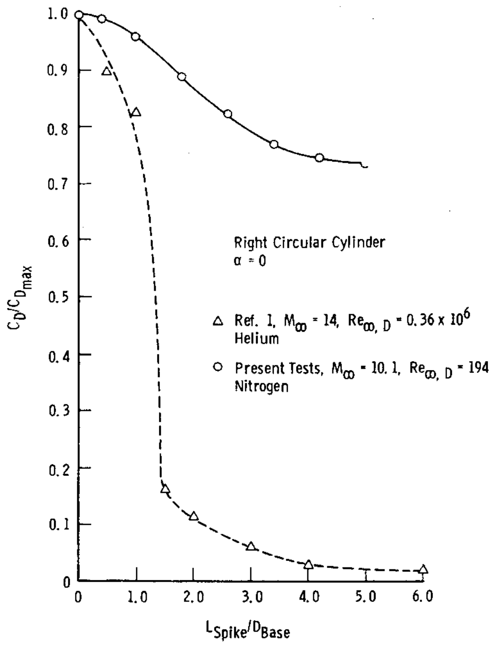

Fig. 4 Drag coefficient ratio, $C_D/C_{D_{max}}$ as a function of spike length.

Correlation of the data for spiked and unspiked bodies in Fig. 3 by using the parameter

$$C_{D*} = (C_D - C_{Di})/(C_{DFM} - C_{Di})$$

(suggested by Potter for use in Ref. 5) indicates that the model shape dependence of C_D is largely removed. This suggests a method for estimating approximate drag coefficients of a wide variety of similar shapes by obtaining inviscid[8] (C_{Di}) and free-molecular[9] (C_{DFM}) drag coefficients and referring to the correlation curve presented herein. Figure 3 shows the correlation of the normalized parameter C_{D*} with the viscous interaction parameter $\bar{V}_\infty$. Included in Fig. 3 are data from Ref. 5, obtained at 0° angle of attack, which have been correlated with the present tests which concerned varying spike lengths ($0 \leq L_{spike}/D_{base} \leq 5$). Because the effects of forebody shape dependence were removed by normalizing the data using the parameter C_{D*}, it is possible to separate the effect of the spike alone and the effect of the change in $\bar{V}_\infty$ caused by the change in body length accompanying addition of the spike.

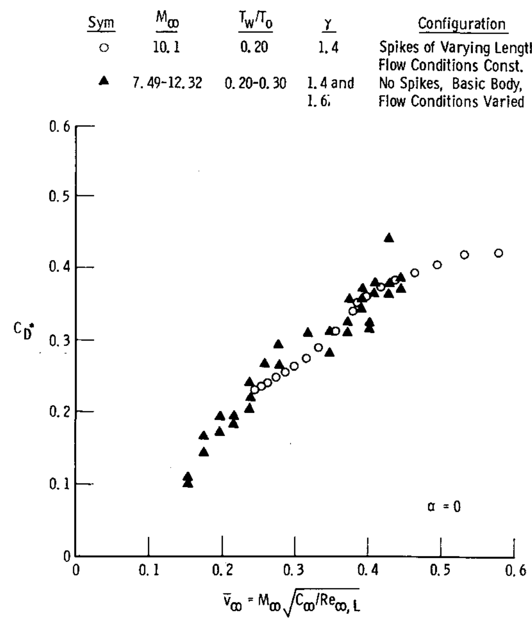

Fig. 3 Normalized drag coefficient, C_{D*} as a function of $\bar{V}_\infty$.

The reduction in drag due to a spike is far less than has been found to occur at high Reynolds numbers. As is noted in earlier studies, for bluff bodies such as the right circular cylinder, drag coefficients may be reduced by more than an order of magnitude in high Reynolds number cases using the sharp spikes. However, as seen in Fig. 4, no such marked reduction occurs for the density altitude simulated here. A 25% reduction is realized, but the length of spike required to accomplish this was $L_{spike} = 5.0\ D_{base}$.

References

[1] Bogdonoff, S. M. and Vas, I. E., "Preliminary investigations of spiked bodies at hypersonic speeds," Wright Air Development Center TN58-7 (March 1958).

[2] Moeckel, W. E., "Flow separation ahead of a blunt axially symmetric body at Mach numbers 1.76 to 2.10," NACA RM E51125 (December 1951).

[3] Album, H. H., "Spiked blunt bodies in supersonic flow," Air Force Office of Scientific Research Rept. 307 (June 1961).

[4] Allen, H. J., "Hypersonic aerodynamic problems of the future," *The High Temperature Aspects of Hypersonic Flow*, edited by W. C. Nelson (Pergamon Press, New York, 1964), pp. 1–41.

[5] Boylan, D. E. and Sims, W. H., "Experimental determination of aerodynamic drag on a blunted 10-deg cone at angles of attack in hypersonic, rarefied flow," Arnold Engineering Development Center TDR-64-60 (April 1964).

[6] Sims, W. H. and Hahn, J. S., "Aerodynamic drag on spiked blunt bodies in low-density hypersonic flow," Arnold Engineering Development Center TDR-64-160 (July 1964).

[7] Potter, J. L., "Low-density, hypersonic (LDH) wind tunnel L," *ARO, Inc., Technical Developments*, edited by J. Lukasiewicz, (ARO, Inc., Arnold Air Force Station, Tenn., 1964), pp. 61–63.

[8] Clark, E. L. and Trimmer, L. L., "Equations and charts for the evaluation of the hypersonic aerodynamic characteristics of lifting configurations by the Newtonian theory," Arnold Engineering Development Center TDR-64-25 (March 1964).

[9] Sentman, L. H., "Free molecule flow theory and its application to the determination of aerodynamic forces," Lockheed Missile and Space Co., Rept. 448514 (October 1961).